Analyzing 6G Satellite IoT Architecture Using Stochastic Geometry: A Meta Distribution Approach

Baly Naganjani*, Ayush Kumar Dwivedi†, Sachin Chaudhari*, and Taneli Riihonen†
*International Institute of Information Technology Hyderabad (IIITH), India
†Faculty of Information Technology and Communication Sciences, Tampere University, Finland
email: baly.naganjani@research.iiit.ac.in, ayush.dwivedi@tuni.fi

***Abstract*—This paper uses 3D stochastic geometry to analyse the coverage and meta-distribution (MD) performance of a low Earth orbit (LEO) satellite-based Internet-of-Things (IoT) network. The satellites are considered to be distributed at a fixed altitude around Earth following a Binomial point process. An IoT device broadcasts its sensed information to all the satellites with a line-of-sight within the visibility region and they act as selective decode-and-forward gateways. The ground server coherently combines the information received from multiple satellites. The analytically derived performance measures are verified through Monte Carlo simulations. The results demonstrate the impact of mega-LEO constellations on coverage and reliability, guiding 6G architecture design to improve connectivity and data offloading in smart cities and dense urban environments.**

***Index Terms*—Internet-of-Things, low Earth orbit constellation, meta distribution, stochastic geometry, 6G architecture.**

I. Introduction

In recent years, the Internet of Things (IoT) has emerged as a transformative technology, promising to connect billions of devices and revolutionize various sectors, from smart cities to industrial automation. However, providing reliable and ubiquitous connectivity for IoT devices remains a significant challenge, especially in dense urban environments or remote areas. Traditional terrestrial networks often struggle to meet the coverage demands of IoT applications. The Low-Earth-orbit (LEO) satellite constellations have gained considerable attention as a potential solution to this connectivity challenge, providing global coverage. LEO satellite networks offer several advantages over traditional geostationary satellites, including lower latency, reduced path loss, and improved global coverage. Satellites are also proposed to be included as a native component in the 6G architecture at the 3rd Generation Partnership Project (3GPP) [1].

Satellite-based IoT networks employ various topologies to enhance connectivity, coverage, and reliability. The star-of-star topology is particularly popular for IoT applications, leveraging the visibility of multiple satellites within a mega-LEO constellation. Similar topologies were proposed in [2], [3] and [4], where satellites serve as transparent or regenerative gateways, forwarding information to a ground server (GS). Regenerative gateways, acting as decode-and-forward (DF) relays, offer higher gains than transparent relays by removing noise before transmission, depending on decoding performance. Similar DF relays are used in terrestrial networks, such as the integrated access backhaul nodes introduced in Release 16 [5], [6]. The performance of such relay networks is usually characterized by the outage or success probability relative to a signal-to-noise ratio (SNR) threshold. In [2], [3], the performance was analyzed considering satellites to be at fixed locations. However, to generalize the analysis over any constellation, tools from stochastic geometry have been applied in [7], [8] to characterize the distribution of satellites using binomial point process (BPP) and nonhomogenous Poisson point process, respectively. Stochastic geometry was also applied to IoT scenarios in [4].

The stochastic geometry, in its basic form, provides only an average performance across all network configurations, offering limited insight into the variability of performance across individual links. Therefore, to overcome this limitation and reveal the distribution of success probabilities across different network realizations, a fine-grained analysis using the concept of meta-distribution (MD) was introduced in [9]. The MD of SNR corresponds to the complementary cumulative distribution function (CCDF) of conditional coverage probability given any position of the satellite. The MD can be used to assess the reliability and quality of service more effectively by quantifying the proportion of links achieving a certain performance threshold. Previous works have focused on MD for terrestrial networks [9]–[11], or for hybrid satellite-terrestrial networks [12].

This paper focuses on direct-access LEO satellite-based IoT networks, specifically analyzing a star-of-star topology where an IoT device communicates directly with multiple satellites. It derives generalized closed-form expressions for coverage and MD in a selective DF system using maximal-ratio combining (MRC) at the GS, validated by Monte Carlo simulations. The results show that the proposed architecture is feasible with typical IoT transmit power and receiver sensitivity. The MD analysis highlights the importance of selecting system parameters like SNR threshold, number of satellites, and altitude to ensure reliability. The results show that the proposed architecture can achieve high coverage and reliability with 8-10 satellites at altitudes between 800 km and 1400 km, as seen in upcoming mega-LEO constellations like Starlink and OneWeb.

II. System Description

Consider a LEO satellite-based IoT network where an IoT device broadcasts sensed information to S satellites ($s = 1, 2, ..., S$) simultaneously using direct access, as shown in

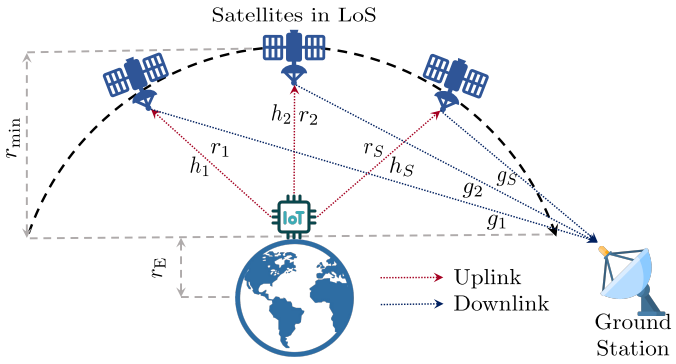

Fig. 1. *System model:* LEO satellites-based IoT network where the device broadcasts its sensed information to all the satellites in LoS, which selectively decodes and forwards the received information to the GS. The GS combines the signals from multiple satellites using MRC.

Fig.1. This system employs a star-of-star topology, which benefits resource-constrained IoT devices by enabling them to offload information without scheduling or coordination [2]–[4]. Similar to NB-IoT, dedicated sub-carriers are used to avoid interference from other devices in the network. The satellite constellation consists of K satellites deployed at an altitude $r_{\min}$ in circular polar orbits. Using stochastic geometry, the satellites are modelled as being uniformly distributed in a BPP on a sphere, resulting in a random number of visible satellites above the horizon, K_{vis}. At any time, an IoT device can establish a line-of-sight (LoS) with S satellites, with others potentially blocked by terrestrial structures.

The end-to-end transmission takes place in two phases. In the first phase, the IoT devices broadcast their sent information received by S satellites simultaneously. The received signal at the sth satellite from an arbitrary user can be written as

$$y_s = \sqrt{P_d\, \mathcal{G}_d\, \mathcal{G}_s\, (\lambda/4\pi r_s)^{\alpha}}\, h_s x + n_s, \tag{1}$$

where P_d is the transmit power of the IoT device, h_s is the shadowed-Rician (SR) distributed coefficient of the uplink channel from the device to the sth satellite, x is the unit energy information signal, r_s is the random distance from the device to the satellite with the path loss exponent α and n_s is the additive white Gaussian noise (AWGN) with zero mean and variance σ_n^2. Also, $\mathcal{G}_d$ and $\mathcal{G}_s$ are the transmit and the receive antenna gains at the device and the satellite respectively. Therefore, the signal-to-noise ratio (SNR) at the sth satellite can be written as

$$\gamma_s = H_s\, r_s^{-\alpha}, \tag{2}$$

where $H_s = \eta_d |h_s|^2$, and $\eta_d = (P_d/\sigma^2_{n_s})\, \mathcal{G}_d\, \mathcal{G}_s\, (\lambda/4\pi)^{\alpha}$.

In the second phase, satellites forward the decoded signals to the GS using a selective decode-and-forward (DF) scheme with dedicated orthogonal resources, avoiding interference. In this scheme, satellites only forward signals if the SNR received at the satellite exceeds a threshold, T. Therefore, the signal received from the sth satellite at the GS can be written as

$$z_s = \sqrt{P_s\, \mathcal{G}_s\, \mathcal{G}_{\text{GS}}\, (\lambda/4\pi r_g)^{\alpha}}\, g_s u + w_s \tag{3}$$

where P_s is the transmit power of the sth satellite, g_s is the SR-distributed downlink channel coefficient, r_g is the distance from the satellite to the GS with path loss exponent α, u is the unit energy signal forwarded by the satellite, and w_s is the AWGN with zero mean and variance σ_w^2. $\mathcal{G}s$ and $\mathcal{G}_{\text{GS}}$ are the transmit and receive antenna gains at the satellite and GS, respectively. With a store-and-forward architecture [13], $r_g = r_{\min}$, meaning downlink occurs when satellites are above the GS. Signals from each satellite are coherently combined at the GS using maximal ratio combining (MRC), yielding the SNR at the GS as follows:

$$\gamma_g(S) = \sum_{s=1}^{S} G_s \text{ such that } G_s = \begin{cases} \eta_s |g_s|^2, & \gamma_s > T, \\ 0, & \text{otherwise}, \end{cases} \tag{4}$$

where $\eta_s = (P_s/\sigma_w^2)\, \mathcal{G}_s\, \mathcal{G}_{\text{GS}}\, (\lambda/4\pi r_g)^{\alpha}$. It is assumed that perfect channel state information (CSI) is available at the satellites and the GS.

A. Shadowed-Rician Channel Model

Satellite communication links are characterized by SR fading models. The probability density function (PDF) and cumulative distribution function (CDF) of the weighted squared shadowed-Rician (SSR) $H_k = \eta_k |h_k|^2$, are given respectively, by [2]

$$f_{H_k}(q) = \alpha_k \sum_{\kappa=0}^{m_k-1} \frac{\zeta(\kappa)}{\eta_k^{\kappa+1}}\, q^{\kappa} e^{-\left(\frac{\beta_k-\delta_k}{\eta_u}\right)q}, \tag{5}$$

$$F_{H_k}(q) = 1 - \alpha_k \sum_{\kappa=0}^{m_k-1} \frac{\zeta(\kappa)}{\eta_k^{\kappa+1}} \sum_{p=0}^{\kappa} \frac{\kappa!}{p!} \left(\frac{\beta_k-\delta_k}{\eta_u}\right)^{-(\kappa+1-p)} \times q^p e^{-\left(\frac{\beta_k-\delta_k}{\eta_u}\right)q}, \tag{6}$$

where $\alpha_k = ((2b_k m_k)/(2b_k m_k + \Omega_k))^{m_k}/2b_k$, $\beta_k = 1/2b_k$, $\delta_k = \Omega_k/(2b_k)(2b_k m_k + \Omega_k)$ and $\zeta(\kappa) = (-1)^{\kappa}(1 - m_k)_{\kappa}\, \delta_k^{\kappa}/(\kappa!)^2$ in which $(\cdot)_{\kappa}$ is the Pochhammer symbol. Here, $2b_k$ represents the average power of the multipath components, m_k signifies the integer Nakagami-m parameter, and Ω_k denotes the average power of the LoS component.

The CDF of the sum of the n i.i.d. SSR random variables assuming $\eta_n = \eta$ for all n is given in [3] as

$$F_{\gamma(n)}(q) = \frac{(2bm_n)^{m_n}}{(2bm_n + \Omega_n)^{m_n}} \sum_{p=0}^{m_n-n} \frac{(m_n - n)!}{(m_n - n - p)!p!} \times \frac{(2bm_n + \Omega_n)^n \Omega_n^p}{(2bm_n)^{p+n}(n + p - 1)!}\, \Gamma\left(p + n, \frac{qm_n}{\eta(2bm_n + \Omega_n)}\right), \tag{7}$$

where $m_n = n \cdot m$, $\Omega_n = n \cdot \Omega$, (m, b, Ω) are the parameters of individual SSR random variables and $\Gamma(.)$ is the lower incomplete Gamma function.

B. Stochastic Geometry Modelling of Satellite Locations

Given that the satellites are assumed to be distributed on a spherical surface according to a BPP, the distance r between a device and a satellite will be random. The total number of satellites above the horizon K_{vis} would also be random and

depend on the total number of satellites in the constellation K. The CDF $F_R(\mathrm{r})$ and the corresponding PDF $f_R(\mathrm{r})$ for $r_{\min} \leq r \leq r_{\max}$ as given in [4] are

$$F_R(r) = \frac{r^2 - r_{\min}^2}{2\, r_E\, r_{\min}},$$
$$f_R(r) = \frac{r}{r_E\, r_{\min}}, \tag{8}$$

where $r_{\max} = \sqrt{r_{\min}^2 + 2 r_E r_{\min}}$ is the maximum distance from device to satellite. Also, the number of satellites visible above the horizon at a given point in time will be distributed according to a binomial random variable with success probability given in [4] as

$$\mathcal{P} = \frac{r_{\min}}{2\,(r_E + r_{\min})}. \tag{9}$$

Therefore, $\Pr[K_{\text{vis}} \geq S]$, the probability of having at least S satellites above the horizon is given as

$$\Pr[K_{\text{vis}} \geq S] = 1 - \sum_{j=0}^{S-1} \binom{K}{j} \mathcal{P}^j\, (1-\mathcal{P})^{K-j}. \tag{10}$$

III. Meta Distribution Analysis

In this section, the coverage probability and the meta-distribution are defined initially. Later, the key expressions are derived in closed form. The coverage probability, conditioned on a given realization of the satellite locations represented by the CCDF of the end-to-end SNR γ is defined as

$$\overline{F}_{\gamma|R}(T) \triangleq \Pr[\gamma > T | R]\ \Pr[K_{\text{vis}} \geq S]. \tag{11}$$

The MD of SNR is the distribution of the conditional success probability, given the locations of the devices, across different network realizations. Given the conditional coverage probability, the MD of the end-to-end SNR is defined as

$$\overline{F}(\tau; T) \triangleq \Pr[\overline{F}_{\gamma|R}(T) > \tau] \tag{12}$$

where $\tau \in [0,1]$ is called as the reliability threshold. It provides insights into the variability of SNR across devices or scenarios, revealing the proportion of devices achieving a specific SNR threshold and thereby offering a more detailed understanding of system performance beyond the average SNR.

Mathematically, it is intractable to find a closed-form expression for (12) directly. Hence, as shown in [12], a beta approximation is used in this paper to find the closed-form expression for (12). The approximate expression of MD is

$$\overline{F}(\tau; T) \approx 1 - I_\tau(\kappa, \beta), \tag{13}$$

where $I_x(z,w) = (1/B(z,w)) \int_0^x t^{z-1}(1-t)^{w-1}\, dt$ is the regularized incomplete beta function and $B(z,w)$ is the beta function as defined in [14, Eq. 3.380.1, 8.392]. Also, the parameters κ and β are given by

$$\kappa = \frac{M_1 M_2 - M_1^2}{M_1^2 - M_2}, \tag{14}$$

$$\beta = \frac{(1-M_1)\,(M_2 - M_1)}{{M_1}^2 - M_2}, \tag{15}$$

where M_1 and M_2 are the first and second moments of the conditional CCDF $\overline{F}_{\gamma|R}(T)$, derived below.

A. Coverage Probability (1st Moment of Conditional CCDF)

The coverage probability of a selective DF network can be calculated by using combinatorial analysis, as shown in [3]. This method considers all possible states of the network, which result from different combinations of satellites either forwarding or not forwarding the received signal. Consider $\mathbf{S}$ represents the set of indices for all S satellites. Then, there will be $2^S - 1$ unique states with at least one satellite forwarding to the GS. Among these states, consider $\mathbf{F}_i$ represents a subset of $\mathbf{S}$ containing the indices of the satellites forwarding to the GS in the ith state. Then, for a given $\mathbf{F}_i$, $s \in \mathbf{F}_i$ would represent all the satellite indices forwarding to the GS and $s \in \mathbf{S} \setminus \mathbf{F}_i$ would represent all the satellite indices not forwarding to the GS. Using these representations, the conditional coverage probability can be written as

$$\overline{F}_\gamma(T \mid R_1, \ldots, R_S) = \sum_{i=0}^{2^S-1} \underbrace{\left[\prod_{\forall s \in \mathbf{F}_i} \overline{F}_{H_s}\left(T r_s^\alpha \mid r_s\right)\right]}_{\text{forwarding}} \underbrace{\left[\prod_{\forall s \in \mathbf{S}\setminus\mathbf{F}_i} F_{H_s}(T r_s^\alpha \mid r_s)\right]}_{\text{not forwarding}} \times \underbrace{\overline{F}_{\gamma_g(v_i)}(T)}_{\text{downlink}} \Pr[K_{\text{vis}} \geq S], \tag{16}$$

where $v_i = |\mathbf{F}_i|$ represents the number of satellites forwarding to the GS in the ith state equaling the cardinal number of $\mathbf{F}_i$. Hence, the coverage probability, also equal to the first moment of the conditional CCDF for the selective DF network of S satellites, can be written as

$$P_{\text{cov}}(T) = \overline{F}_\gamma(T) = M_1 = \int_{r_1,..,r_S} \cdots \int \overline{F}_\gamma(T \mid R_1, \ldots, R_S) \left(\prod_{s=1}^{S} f_{R_s}(r_s)\right) dr_1 \ldots dr_S. \tag{17}$$

It is obvious that $v_i \in \{1, \cdots, S\}$ and for every possible value of v_i there will be $\binom{S}{v_i}$ possible number of unique $\mathbf{F}_i$. In other words, for a given number of satellites forwarding to the GS, there will be $\binom{S}{v_i}$ possible states or combinations. Hence, if all the uplink channels and the distance between the device and the satellites are identically distributed, (17) can be simplified to give

$$\overline{F}_\gamma(T) = \Pr[K_{\text{vis}} \geq S] \sum_{v=1}^{S} \binom{S}{v} I_1^v\, (1-I_1)^{S-v}\, \overline{F}_{\gamma_g(v)}(T), \tag{18}$$

where $I_1 = \mathbb{E}_R\left[\overline{F}_H(T r^\alpha)\right] = \int_r \overline{F}_H(T r^\alpha) f_R(r)\, dr$, for which a closed form solution is given in Appendix A. Similarly, it can be shown that $\mathbb{E}_R\left[F_H(T r^\alpha)\right] = \int_r F_H(T r^\alpha) f_R(r)\, dr = 1 - I_1$.

$$M_2 = P_{K_{\text{vis}}\geq S}^2 \Bigg\{ \overbrace{\sum_{i=1}^{2^S-1} \left(\int_r \overline{F}_H \left(Tr^\alpha \mid r\right)^2 f_R(r) dr \right)^{v_i} \left(\int_r F_H(Tr^\alpha \mid r)^2 f_R(r) dr \right)^{S-v_i} \overline{F}_{\gamma_g(v_i)}(T)^2}^{\text{square terms}} + 2 \underbrace{\sum_{1\leq i<j\leq 2^S-1} \left(\int_r \overline{F}_H(Tr^\alpha|r)^2 f_R(r) dr \right)^{n_2} \left(\int_r \overline{F}_H(Tr^\alpha|r) F_H(Tr^\alpha|r) f_R(r) dr \right)^{n_1} \left(\int_r F_H(Tr^\alpha|r)^2 f_R(r) dr \right)^{n_0} \overline{F}_{\gamma_g(v_i)}(T) \overline{F}_{\gamma_g(v_j)}(T) \Bigg\}}_{\text{cross product terms}} \tag{21}$$

B. 2nd Moment of Conditional CCDF

The second moment of the conditional CCDF of the end-to-end SNR is given by

$$M_2 = \int_{r_1,..,r_S} \cdots \int \left(\overline{F}_\gamma(T \mid R_1, \ldots, R_S) \right)^2 \left(\prod_{s=1}^{S} f_{R_s}(r_s) \right) dr_1 \ldots dr_S. \tag{19}$$

In (19), the term for the square of the conditional CCDF can be expanded using the multinomial theorem. For example,

$$(x_1 + \cdots + x_n)^2 = \underbrace{\sum_{i=1}^{n} x_i^2}_{\text{square terms}} + 2 \underbrace{\sum_{1\leq i<j\leq n} x_i x_j}_{\text{cross product terms}}. \tag{20}$$

Each x_i or x_j in (20) corresponds to a conditional coverage probability term from 2^S-1 different states of satellites. Using this approach, (19) can be resolved to give (21), where v_i and v_j represent the number of satellites forwarding in the ith and jth states, respectively. Also, n_2 indicates the number of instances where a particular satellite forward in both x_i and x_j terms, n_1 indicates the number of instances where a particular satellite forward in either x_i or x_j term, and n_0 indicates the number of instances where a particular satellite does not forward in both x_i and x_j terms. These can be easily computed by generating all the possible states and the respective combinations for the cross-product terms.

A closed-form expressions for the integral of the form $I_2 = \int \overline{F}_H(Tr^\alpha)^2 f_R(r)\, dr$ is given in Appendix B. Similarly the integral of the form $\int \overline{F}_H(Tr^\alpha|r)\, F_H(Tr^\alpha|r) f_R(r) dr$ can be solved as $(I_1 - I_2)$, and the integral of the form $\int F_H(Tr^\alpha)^2 f_R(r)\, dr$ can be solved as $(1 - 2I_1 + I_2)$. Therefore, the M_2 can be written as

$$M_2 = P_{K_{\text{vis}}\geq S}^2 \Bigg\{ \sum_{i=1}^{2^S-1} I_2^{v_i} \left(1 - 2I_1 + I_2\right)^{S-v_i} \overline{F}_{\gamma_g(v_i)}(T)^2 + 2 \sum_{1\leq i<j\leq 2^S-1} I_2^{n_2} \left(I_1 - I_2\right)^{n_1} \left(1 - 2I_1 + I_2\right)^{n_0} \overline{F}_{\gamma_g(v_i)}(T)\, \overline{F}_{\gamma_g(v_j)}(T) \Bigg\}. \tag{22}$$

Using (18) and (22) together with (14) and (15) in (13) gives the closed-form expression of the MD of the end-to-end SNR.

IV. Numerical Results and Observations

In this section, the theoretical and simulation results of coverage and MD as a function of SNR threshold T, reliability threshold τ, the altitude r_{min} are discussed. The simulations are performed for 10^4 channel realizations using MATLAB. The channels between all users and the satellites are assumed to be heavy-shadowed with parameters $m = 1$, $b = 0.063$, $\Omega = 0.0007$. Whereas the channel between the satellites and the GS is assumed to be average shadowed with parameters $m = 5$, $b = 0.251$, $\Omega = 0.279$. Unless stated otherwise, $r_{\text{E}} = 6371$ km, $r_{\text{min}} = 600$ km, $\alpha = 2$, $P_u = 26$ dBm, $P_s = 40$ dBm, $\sigma_n^2 = -121.44$ dBm, $\sigma_w^2 = -98$ dBm, $B = 180$ kHz, $f = 2$ GHz, device antenna transmit gain $\mathcal{G}_d = 0$ dBi, satellite antenna transmit/receive gain $\mathcal{G}_s = 24$ dBi, and GS receive antenna gain $\mathcal{G}_{\text{GS}} = 30$ dBi.

Fig. 2 shows the coverage probability $\overline{F}(T)$ and variance $M_2 - (M_1)^2$ of the CCDF of end-to-end SNR as a function of SNR threshold T for different satellite numbers. Theoretical and simulated values match, confirming the accuracy of the derivation for moments M_1 and M_2. The coverage probability decreases with higher SNR thresholds but improves with more satellites. For example, at $T = 0$ dB, coverage improves from 0.5 to 0.8 by increasing satellites from 2 to 5, demonstrating the benefit of a mega-LEO constellation. However, at $T > 10$ dB, even with $S = 8$, coverage eventually decreases, indicating a limit to satellite addition. For LoRaWAN-based satellite-IoT, an SNR threshold between -6 dB to -20 dB is needed to maintain a BER of 10^{-5}, resulting in receiver sensitivity between -123 dBm and -137 dBm [15]. Similarly, for NB-IoT, sensitivity is typically between -130 dBm and -140 dBm [16]. Notably, with 5 and 8 satellites, high coverage probability is achievable for SNR thresholds up to 0 dB, well within the desired range.

Fig. 2 also shows the variance of the conditional CCDF as the SNR threshold increases. This variance reflects the SNR spread experienced by devices across different satellite locations, indicating the fairness between individual links. A low variance (< 0.06) suggests consistent performance across the network, with most devices experiencing similar SNR levels. The variance is zero at extreme SNR thresholds ($T \to -\infty$ or $T \to \infty$) and slightly peaks at some finite SNR thresholds. As the number of satellites increases, variance also increases due to more potential relay options, leading to greater SNR fluctuations. However, adding more satellites raises the likelihood of successful signal forwarding by at least one satellite. Consequently, to maintain a target variance, the SNR threshold can be lowered. Essentially, more satellites make it easier to

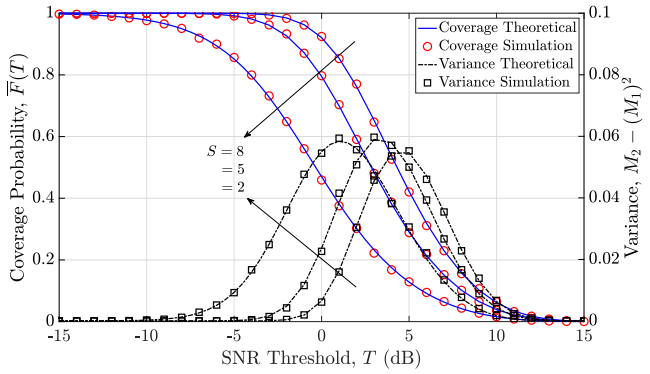

Fig. 2. Coverage probability $\overline{F}(T)$ (first moment M_1) and the variance $(M_2 - M_1^2)$ of the conditional CCDF of the end-to-end SNR (γ) vs the SNR threshold T (dB) for varying number of satellites S.

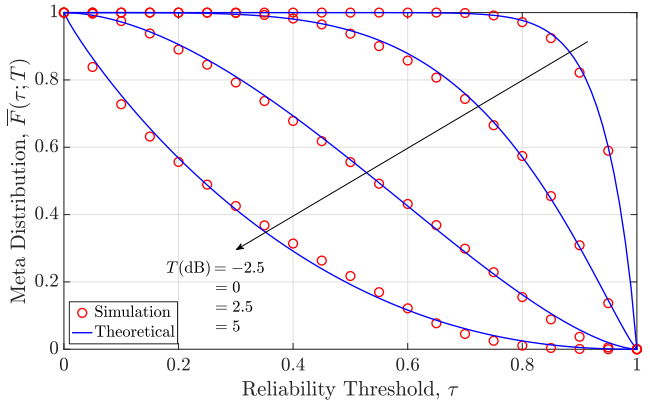

Fig. 3. Meta distribution $\overline{F}(\tau;T)$ vs reliability threshold τ for $S = 5$ and varying SNR threshold T.

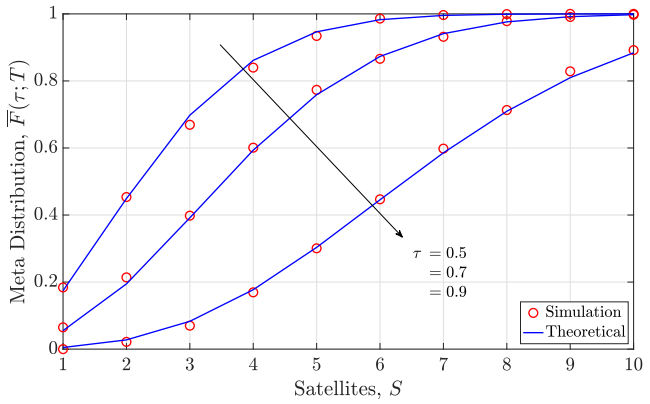

Fig. 4. Meta distribution $\overline{F}(\tau;T)$ vs number of satellites (S) for varying reliability threshold τ at $T = 0$ dB.

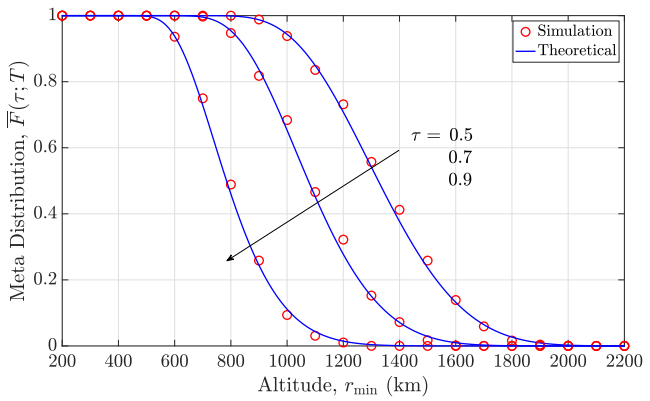

Fig. 5. Meta distribution $\overline{F}(\tau;T)$ vs altitude of the satellites $r_{\min}$ (km) for varying reliability threshold τ at $T = 0$ dB.

achieve a certain level of SNR, reducing the required threshold to maintain the same variance in performance.

Fig. 3 shows impact of T on MD $\overline{F}(\tau;T)$ for various τ with $S = 5$. The simulations closely match the theoretical values, indicating that the beta approximation provides a tight fit for the MD. It can be observed that the MD decreases as T increases. This behavior shows that higher T reduces the number of links capable of achieving the desired SNR. For instance, at $T = 2.5$ dB and $\tau = 0.5$, MD is approximately 0.6, which means that 60% of user-satellite-GS links can achieve an SNR of 2.5 dB with at least 50% probability. Furthermore, it can be observed that reliability is highly sensitive to minor increases in T. For example, as T increases from 0 dB to 2.5 dB, there is a noticeable drop in the curve, especially for higher values of τ. This fine-grained analysis highlights the critical importance of carefully selecting T to maintain desired reliability levels in the network.

Fig. 4 illustrates the meta distribution $\overline{F}(\tau;T)$ as a function of S for various reliability thresholds $\tau = 0.5, 0.7$, and 0.9. MD increases as S increases across all the values of reliability threshold τ, implying that adding more satellites enhances the reliability of the system. The system achieves a reliability close to 1 when $\tau = 0.5$ with approximately 6 satellites. For $\tau = 0.9$, the system needs around 9 to 10 satellites to approach good reliability. For instance, moving from 3 to 5 satellites under $\tau = 0.7$ leads to a 40% boost in reliability, which is achievable in the mega-LEO constellation. However, the increase from 8 to 10 satellites results in a merely 10% boost in reliability implying that beyond a certain point, adding more satellites improves reliability only marginally.

Fig. 5 illustrates the relation between the altitude $r_{\min}$ and MD for various τ. It can be observed that a desirable MD can be achieved across a specific range of altitude values. Specifically for $\tau = 0.5$, a required MD (close to 1) is attained for a range of altitudes between 600 km and 1000 km, indicating that the system model is suitable for LEO constellations. For $\tau = 0.7$, it is observed that MD greater than 0.5 is maintained within altitude range of approximately 800 km to 1400 km, which is considered a good range for deploying constellation, as it provides a robust trade-off between altitude and coverage.

V. Conclusion

This paper analyzes coverage and meta-distribution in a satellite IoT network using multiple satellites, modelled through stochastic geometry. The meta-distribution analysis highlights the importance of carefully selecting system parameters like signal quality thresholds, satellite count, and

altitude to ensure high reliability. The results show that the proposed architecture's ability to achieve high coverage and reliability aligns well with the capabilities of mega-LEO satellite constellations, making it suitable for future low-power IoT networks. In the future, this analysis can be extended to account for interference from other networks.

APPENDIX A
CLOSED-FORM EXPRESSION FOR THE INTEGRAL I_1

To find the closed form expression for the integral $\int_r \overline{F}_H(Tr^\alpha) f_R(r)\, dr$, consider using (6) and (8) as follows:

$$\begin{aligned}
&\int_r \overline{F}_H(Tr^\alpha) f_R(r)\, dr \\
&= \int_{r_{\min}}^{r_{\max}} \left[\alpha_k \sum_{\kappa=0}^{m_k-1} \frac{\zeta(\kappa)}{\eta_u^{\kappa+1}} \sum_{p=0}^{\kappa} \frac{\kappa!}{p!} (Tr^\alpha)^p \left(\frac{\beta_k - \delta_k}{\eta_u} \right)^{-(\kappa+1-p)} \right. \\
&\quad \left. \times e^{-\left(\frac{\beta_k-\delta_k}{\eta_u}\right) Tr^\alpha} \right] \left(\frac{r}{r_e r_{\min}} \right) dr \\
&\overset{(a)}{=} \alpha_k \sum_{\kappa=0}^{m_k-1} \frac{\zeta(\kappa)}{\eta_u^{\kappa+1}} \sum_{p=0}^{\kappa} \frac{\kappa!}{p!} \left(\frac{\beta_k - \delta_k}{\eta_u} \right)^{-(\kappa+1-p)} \frac{T^p}{r_e r_{\min}} \\
&\quad \times \int_{r_{\min}}^{r_{\max}} r^{\alpha p+1} e^{-\left(\frac{\beta_k-\delta_k}{\eta_u}\right) Tr^\alpha} dr \\
&\overset{(b)}{=} \alpha_k \sum_{\kappa=0}^{m_k-1} \frac{\zeta(\kappa)}{\eta_u^{\kappa+1}} \sum_{p=0}^{\kappa} \frac{\kappa!}{p!} A_k^{-(\kappa+1-p)} \frac{T^p}{r_e r_{\min}} \\
&\quad \times \left[\left(\frac{\gamma\left(\overline{p}, A_k\, T\, r_{\max}^\alpha\right)}{\alpha\ (A_k T)^{\overline{p}}} \right) - \left(\frac{\gamma\left(\overline{p}, A_k\, T r_{\min}^\alpha\right)}{\alpha\ (A_k T)^{\overline{p}}} \right) \right], \qquad (23)
\end{aligned}$$

where the integral in (a) is solved using [14, Eq. 3.381.8], and the terms $A_k = \left(\frac{\beta_k-\delta_k}{\eta_u}\right)$ and $\overline{p} = p + \frac{2}{\alpha}$ are used for concise representation in (b). Here $\gamma(\cdot,\cdot)$ represents the lower incomplete Gamma function [14, Eq. 8.350.1].

APPENDIX B
CLOSED-FORM EXPRESSION FOR THE INTEGRAL I_2

To find the closed form expression for the integral $\int_r (\overline{F}_H(Tr^\alpha))^2 f_R(r)\, dr$, consider using (6) and (8) as follows:

$$\begin{aligned}
&\int_{r_{\min}}^{r_{\max}} (\overline{F}_H(Tr^\alpha))^2 f_R(r)\, dr \\
&= \int_{r_{\min}}^{r_{\max}} \left[\alpha_k \sum_{\kappa=0}^{m_k-1} \frac{\zeta(\kappa)}{\eta_u^{\kappa+1}} \sum_{p=0}^{\kappa} \frac{\kappa!}{p!} (Tr^\alpha)^p \left(\frac{\beta_k - \delta_k}{\eta_u} \right)^{-(\kappa+1-p)} \right. \\
&\quad \left. \times e^{-\left(\frac{\beta_k-\delta_k}{\eta_u}\right) Tr^\alpha} \right]^2 \left(\frac{r}{r_e r_{\min}} \right) dr \\
&\overset{(a)}{=} \int_{r_{\min}}^{r_{\max}} \alpha_k^2 e^{-2A_k(Tr^\alpha)} \sum_{\rho(2,m_k)} \binom{2}{q_0, \ldots, q_{m_k}-1} \prod_{t=0}^{m_k-1} {S_t}^{q_t} \\
&\quad (Tr^\alpha)^{\sum_{\kappa=0}^{m_k-1} \kappa q_k} \left(\frac{r}{r_e r_{\min}} \right) dr \\
&\overset{(b)}{=} \frac{\alpha_k^2}{r_e r_{\min}} \sum_{\rho(2,m_k)} \mathbb{C}_q^2 \left(\prod_{t=0}^{m_k-1} {S_t}^{q_t} \right) T^{\sum_{\kappa=0}^{m_k-1} \kappa q_\kappa} \\
&\quad \times \int_{r_{\min}}^{r_{\max}} r^{\alpha(\sum_{\kappa=0}^{m_k-1} \kappa q_\kappa)+1} e^{-2A_k T r^\alpha} dr. \\
&= \frac{\alpha_k^2}{r_e r_{\min}} \sum_{\rho(2,m_k)} \hat{S}\, T^{\sum_{\kappa=0}^{m_k-1} \kappa q_\kappa} \\
&\quad \times \left[\frac{\gamma\left(\widetilde{q}, 2A_k T r_{\max}^\alpha\right)}{\alpha\left(2A_k T\right)^{\widetilde{q}}} - \frac{\gamma\left(\widetilde{q}, 2A_k T r_{\min}^\alpha\right)}{\alpha\left(2A_k T\right)^{\widetilde{q}}} \right], \qquad (24)
\end{aligned}$$

where multinomial theorem is applied in (a) to resolve the terms in the summation running over the values of κ with $\rho(2, m_k) \triangleq \{q_0, \ldots, q_{m_k-1} : q_t \in \mathbb{N}, \sum_{t=1}^{m_k-1} q_t = 2\}$. Also, $\hat{S} = \mathbb{C}_q^2 \left(\prod_{t=0}^{m_k-1} {S_t}^{q_t} \right)$, $\mathbb{C}_q = \binom{2}{q_0, \ldots, q_{m_k}-1}$, $S_t = \frac{1}{t!} \left(\frac{\beta_k-\delta_k}{\eta_u} \right)^t \sum_{\kappa=t}^{m_k-1} \frac{\zeta(\kappa)}{\eta_u^{\kappa+1}} \left(\frac{\beta_k-\delta_k}{\eta_u} \right)^{-(\kappa+1)} (\kappa!)$, and $\widetilde{q} = (\sum_{\kappa=0}^{m_k-1} \kappa q_\kappa) + \frac{2}{\alpha}$.

REFERENCES

[1] ETSI conference on "Non-Terrestrial Networks, a native component of 6G", "Vision on Non-Terrestrial Networks in 6G system (or IMT-2030) ," *6G-NTN White Paper*, 2024.

[2] A. K. Dwivedi, S. Praneeth Chokkarapu, S. Chaudhari, and N. Varshney, "Performance analysis of novel direct access schemes for LEO satellites based IoT network," in *IEEE 31st Annu. Int. Symp. Pers., Indoor, Mobile, Radio Commun. (PIMRC)*, 2020.

[3] N. Lamba, A. K. Dwivedi, and S. Chaudhari, "Performance analysis of selective decode-and-forward relaying for satellite-IoT," in *2022 IEEE Globecom Workshops (GC Wkshps)*, 2022, pp. 1127–1132.

[4] A. K. Dwivedi, S. Chaudhari, N. Varshney, and P. K. Varshney, "Performance analysis of LEO satellite-based IoT networks in the presence of interference," *IEEE Internet of Things Journal*, pp. 1–1, 2023.

[5] 3rd Generation Partnership Project (3GPP); Technical Specification Group Radio Access Network, "Study on Integrated Access and Backhaul (Rel 16)," *TR 38.874V16.0.0*, 2018.

[6] S. Gadhai and R. Budhiraja, "Evolution of network nodes: From IAB to IRS," *3GPP Highlights Newsletter Issue 06*, 2024, (Accessed 21 Jun. 2024). [Online]. Available: https://www.3gpp.org/newsletter-issue-06-may-2023#flipbook-flip7/21/

[7] N. Okati, T. Riihonen, D. Korpi, I. Angervuori, and R. Wichman, "Downlink coverage and rate analysis of low earth orbit satellite constellations using stochastic geometry," *IEEE Trans. on Commun.*, vol. 68, no. 8, pp. 5120–5134, 2020.

[8] N. Okati and T. Riihonen, "Nonhomogeneous Stochastic Geometry Analysis of Massive LEO Communication Constellations," *IEEE Trans. on Commun.*, vol. 70, no. 3, pp. 1848–1860, 2022.

[9] M. Haenggi, "The Meta Distribution of the SIR in Poisson Bipolar and Cellular Networks," *IEEE Trans. on Wireless Commun.*, vol. 15, no. 4, pp. 2577–2589, 2016.

[10] H. Ibrahim, H. Tabassum, and U. T. Nguyen, "The Meta Distributions of the SIR/SNR and Data Rate in Coexisting Sub-6GHz and Millimeter-Wave Cellular Networks," *IEEE Open J. of the Commun. Society*, vol. 1, pp. 1213–1229, 2020.

[11] M. Shi, X. Gao, K. Yang, D. Niyato, and Z. Han, "Meta distribution of the SINR for mmWave cellular networks with clusters," *IEEE Trans. on Commun.*, vol. 69, no. 10, pp. 6956–6970, 2021.

[12] H. Lin, C. Zhang, Y. Huang, R. Zhao, and L. Yang, "Fine-grained analysis on downlink LEO satellite-terrestrial mmWave relay networks," *IEEE Wireless Commun. Lett.*, vol. 10, no. 9, pp. 1871–1875, 2021.

[13] Lacuna Space Ltd., *An ultra-low cost sensor service for small amounts of data*, (Accessed 20 Aug. 2024). [Online]. Available: https://lacuna-space.com/about/

[14] I. Gradshteyn and I. Ryzhik, "Tables of integrals, series and products," *New York: Academic Press*, 2000.

[15] M. A. B. Temim, "Low-earth-orbit satellite communications using LoRa-like signals," Ph.D. dissertation, Université de Bordeaux, 2022.

[16] M. Idrissi, *3GPP Release 17: Understanding NB-IoT over NTN*, (Accessed 20 Aug. 2024). [Online]. Available: https://5ghub.us/3gpp-release-17-understanding-nb-iot-over-ntn/